Published in final edited form as:
Genesis. 2011 April ; 49(4): 326–341. doi:10.1002/dvg.20714.

The role of sensory organs and the forebrain for the development of the craniofacial shape as revealed by *Foxg1-cre* mediated microRNA loss

Jennifer Kersigo[1], **Alex D'Angelo**[1], **Brian Gray**[2], **Garrett A. Soukup**[3], and **Bernd Fritzsch**[1]

[1] University of Iowa, Department of Biology, Iowa City, IA

[2] Molecular Targeting Technologies, Inc., Westchester, PA

[3] Creighton University, Department of Biomedical Sciences, Omaha, NE

Abstract

Cranial development is critically influenced by the relative growth of distinct elements. Previous studies have shown the transcription factor *Foxg1* to be expressed is essential for development of telencephalon, olfactory epithelium, parts of the eye and the ear. Here we investigate the effects of a *Foxg1-cre* mediated conditional deletion of *Dicer1* and microRNA (miRNA) on mouse embryos. We report the rapid and complete loss of the telencephalon and cerebellum as well as severe reduction in the ears and loss of the anterior half of the eyes. These losses result in unexpectedly limited malformations of anterodorsal aspects of the skull. We investigated the progressive disappearance of these initially developing structures and found a specific miRNA of nervous tissue, miR-124, to disappear prior to reduction in growth of the specific neurosensory areas. Correlated with the absence of miR-124, these areas showed numerous apoptotic cells that stained positive for anti-cleaved caspase 3 and the phosphatidylserine stain PSVue prior to the near or complete loss of those brain and sensory areas (forebrain, cerebellum, anterior retina, ear). We conclude that *Foxg1-cre* mediated conditional deletion of *Dicer1* leads to absence of functional miRNA followed by complete or nearly complete loss of neurons. Embryonic neurosensory development therefore depends critically on miRNA. Our data suggest that loss of a given neuronal compartment can be triggered using early deletion of *Dicer1* and thus provides a novel means to genetically remove specific neurosensory areas to investigate loss of their function on morphology (this study) or signal processing within the brain.

Keywords

forebrain; cerebellum; eye; ear; conditional deletion; cre

Introduction

The evolution of the vertebrate head hinges on the evolution of the three major long distance sensory systems (eye, ear and nose), the jaws and the brain. In particular the increased size of the forebrain (Nieuwenhuys et al., 1998) changes the appearance of the head in man compared to other mammals and non-mammalian vertebrates. Moreover, the olfactory inlet with the conchae covered with sensory epithelium and the eye surrounded by a bony orbit determine, as constructional elements, the shape of the human and vertebrate skull. The

Corresponding author: Dr. Bernd Fritzsch, Department of Biology, University of Iowa, Iowa City, IA, 52242, Tel: 319-353-2969, Fax: 319-335-1069, bernd-fritzsch@uiowa.edu.

inner ear is a major constructional component of the skull forming with the petrous bone one of the strongest bones in the human body with which many other skull bones are fused. Evolution of the brain and the major sensory systems predates the formation of the jaws, as all jawless fishes already have all three sensory systems and a brain with the same subdivisions as typically found in jawed vertebrates (Fritzsch and Glover, 2006; Nieuwenhuys, 2002). Recent data have implicated several diffusible factors as playing a quantitative role in the development of specific skull or brain regions. For example, sonic hedgehog signaling is important for the growth of the forebrain, upper jaw and eye, and their size is regulated by levels of sonic hedgehog expression (Young *et al.*, 2010). In an attempt to reveal the contribution of distinct compartments on overall head morphology we followed here a novel route, genetically ablating entire structures by conditionally deleting the microRNA (miRNA) generating enzyme Dicer1 to assess the importance of these sensory and neuronal components for craniofacial development in a mouse embryo.

We previously showed (Soukup et al., 2009) that deletion of all small RNAs in the developing ear by conditionally deleting *Dicer1* results in reduction of neurosensory development. Others recently demonstrated that depletion of floxed *Dicer1* using *Wnt1-cre* results in loss of neural crest-derived tissue and cranio-facial malformation (Huang *et al.*, 2010). Later ablation of floxed *Dicer1* in neurons results in variable defects and sometimes no effect at all (Hebert *et al.*, 2010), leaving open the possibility of uniform neuronal defects after depletion of floxed *Dicer1* with various *cre* lines. Indeed, reduction of the neurosensory part of the ear was incomplete with the *Pax2-cre* line possibly due to incomplete recombination in the posterior canal crista and the cochlea, both of which showed some hair cell development and few neurons that innervated those endorgans. We also found that the dorsal part of the midbrain and the cerebellum, both of which express *Pax2-cre* (Ohyama and Groves, 2004), undergo massive neuronal degeneration after the floxed *Dicer1* has been eliminated (Soukup et al., 2009) and this neuronal loss was confirmed recently using *Wnt1-cre* (Huang *et al.*, 2010). In contrast, the kidney, which also expresses *Pax2-cre*, and has complete recombination of the floxed *Dicer1* showed a substantial reduction in size but no complete loss (Soukup et al., unpublished observations). These data suggest that neuronal and neurosensory differentiation may be more dependent on the action of Dicer1-dependent mature small RNA as recently proposed for several other brain areas (Shi *et al.*, 2010). We reasoned that it should be possible to eliminate all neurosensory and brain development using a *cre* line that is expressed in forebrain, olfactory system, retina and ear while maintaining the surrounding non-neuronal tissue as this would respond less to the absence of miRNAs thereby revealing the effect these structures have on overall cranio-facial morphology.

Among the small number of possible genes that show such widespread expression we chose the winged helix (WH) gene Forkhead Box G1 (*Foxg1*, previously BF1). This gene is expressed early and widespread in the forebrain, olfactory epithelium, medial half of the retina, the ear, and shows limited expression in multiple non-neuronal tissues (Clevidence et al., 1993; Hatini et al., 1994). Null mutations for this gene showed that *Foxg1* is necessary for proper cortical development in the embryonic telencephalon (Hanashima et al., 2002). When *Foxg1* is absent in the developing cortex of mouse brains, the earliest-born neurons are observed in abundance when compared to the wild-type (WT) mice, indicating the role of *Foxg1* in suppressing neuronal progenitor cell fate through transcriptional repression (Hanashima et al., 2004). *Foxg1* null mutants have been shown to exhibit a shrunken dorsal telencephalon due to an increased rate of neuronal progenitor cell differentiation. This results in a decreased number of progenitor cells in the cell cycle able to proliferate (Xuan et al., 1995). *Foxg1* also leads to a loss of sensorineural differentiation in the ears of *Foxg1* null mice, in particular in the cochlea, which is reduced to a simple half turn (Pauley et al., 2006), affects the anterior part of the eye and is necessary for olfactory system development

(Duggan *et al.*, 2008; Kawauchi *et al.*, 2009). An mutation of *Foxg1* exists in which the coding frame of *Foxg1* has been replaced by *cre*, thus allowing expression of *cre* in all cells that express *Foxg1* (Hebert and McConnell, 2000). Several papers have meanwhile demonstrated that the *Foxg1-cre* can be used effectively to recombine floxed genes in eyes, ears, olfactory system and forebrain and other aspects of the developing and mature brain (Shi *et al.*, 2010), thus validating that the *Foxg1-cre* can have such a widespread effect on floxed genes.

Here we examine the effects of a *Foxg1-cre* mediated conditional deletion of *Dicer1*, a gene that generates the lead enzyme to form active miRNAs (Hebert *et al.*, 2010; Soukup *et al.*, 2009), on the brains, eyes, ears and the olfactory epithelium of mice. In all developing mutant neurosensory systems we observe rapid dissolution of structures through cell death of the forebrain, the cerebellum, the anterior half of the retina, the olfactory epithelium and the ear. At the macroscopic level the forebrains are missing, the eyes are reduced, and the ear and olfactory epithelia are nearly lost by E18.5. We investigated the incidence of cell death in these structures using immunochemistry of anti-cleaved caspase 3 as well as a novel stain for phosphatidylserine (PS) staining in dying cells, PSVue (MTTI Research). We found that only disappearing tissues displayed marked increases in anti-cleaved caspase 3 expression and PSVue staining, indicating higher levels of cell death in the *Foxg1-cre::Dicer1*$^{f/f}$ conditional null mutant. Our results demonstrate the selective dependency of neuronal development on active miRNAs and other small RNAs. The topology of these effects is consistent with *Foxg1* expression, but is much more severe than those reported in *Foxg1* mutant mice (Kawauchi *et al.*, 2009; Pauley *et al.*, 2006; Xuan *et al.*, 1995): the *Foxg1-cre* mediated *Dicer1* deletion results in complete loss of the telencephalon and olfactory bulbs within a few days. Of note is the cerebellum's failure to develop, as its development has previously been unrecognized as being *Foxg1*-dependent.

Materials and Methods

Mouse model and genotyping

To generate the conditional *Dicer1* knockout mice (CKO), *Foxg1*-cre::*Dicer1*$^{f/f}$, we crossed the *Foxg1-cre* line (Hebert et al., 2000; 129(Cg)-*Foxg1*$^{tm1(cre)Skm}$/J) with the floxed *Dicer1* (Harfe et al., 2005; *Dicer1*^{tm1Bdh}/J). *Foxg1-cre::Dicer1*$^{f/f}$ were used as the conditional knockout (CKO) mutants and litter mate *Foxg1-cre:: Dicer1*$^{f/+}$ and *Dicer1*$^{f/f}$ were used as wild type controls (WT). The mice were genotyped by PCR analysis of tail DNA under standard conditions with *Dicer1* specific primers (IMR6305: 5′-CCT GAC AGT GAC GGT CCA AAG-3′; IMR6569: 5′-CAT GAC TCT TCA ACT CAA ACT-3′) which yielded a mutant band at 420bp and a wild type band at 351bp, and general *cre* primers (Cre1: 5′-CCT GTT TTG CAC GTT CAC CG-3′; Cre3: 5′-ATG CTT CTG TCC GTT TGC CG-3′) which yielded a band at 280bp.

Embryos were collected from pregnant dams at embryonic days (E) 10.5, 11.5, 12.5, 14.5, 16.5, and 18.5 with noon the day of vaginal plug visualization considered embryonic day 0.5. To collect embryos, pregnant dams were anesthetized with 1.25% Avertin at a dose of 0.025ml/g by IP injection. Embryos were dissected from the uterus and perfusion fixed with 4% PFA in 0.1M phosphate buffer (pH 7.4). All animal care and procedures were approved by the University of Iowa Institutional Animal Care and Use Committee (ACURF 0804066).

In Situ hybridization

Whole mount *in situ* hybridization experiments were conducted using a locked nucleic acid (LNA) probe labeled with digoxigenin (Roche) purchased from Exiqon (mmu-miR-124; 39452-05) as described before (Jahan *et al.*, 2010; Soukup *et al.*, 2009). Briefly, 2 samples at

various stages of wild type CKO mice were fixed in 4% paraformaldehyde (PFA), dissected in 0.4% PFA under RNase-free conditions, defatted and then rehydrated in a graded methanol series, digested with proteinase K (Ambion), and then hybridized to the miR-124 LNA probe overnight at 60°C. Unbound probe was washed off and the tissue was incubated overnight with anti-digoxigenin antibody (Roche) conjugated with alkaline phosphatase (AP) at room temperature. The LNA probe was detected using BM Purple AP Substrate (Roche). The tissue was mounted in glycerol and imaged with a Nikon E800 microscope.

Immunochemistry

At least 2 samples per stage and genotype were fixed in 4% paraformaldehyde (PFA) for at least 12 hours prior to at least 1 hour of dehydration in 70% ethanol. They were then rehydrated incrementally by adding phosphate-buffered saline (PBS). This was followed by blocking for 1 hour in 2.5% normal goat serum (NGS) and 0.5% Triton X-100 at room temperature (RT) on a shaker. After blocking, samples were washed briefly with PBS, and then allowed to incubate for 72 hours on a shaker at 4°C with primary antibodies (anti-acetylate β-tubulin 1:800, Sigma; anti-cleaved caspase 3 1:100, Cell Signaling Technology; anti-myosin 7a 1:200, Proteus Biosciences; anti-cre 1:100, Covance) at proper dilution in block solution. Samples were then washed 3 times with PBS over 1 hour, and then placed in blocking solution for 1 hour. Secondary antibodies (Alexa fluor molecular probe 633, 532, or 488; Invitrogen) were then added at 1:500 dilution in block solution and allowed to incubate for at least 24 hours at 4°C on a shaker. The samples were washed with Hoechst stain for 1 hour by diluting 10mg/ml stock (Polysciences, Inc. Hoechst Dye 33258) 1:2000 in PBS. Samples were then washed 2–3 times with PBS at RT on a shaker. Some samples were labeled further with PSVue480/550 apoptotic cell stain (see below for method). Samples were mounted in glycerol. Images were taken with a Leica TCS SP5 confocal microscope.

Apoptotic cell labeling

Apoptotic cells were labeled using the PSVue480 or 550 cell stain following the recommended procedure (Molecular Targeting Technologies, Inc.). Briefly, a 2 mM solution of pre-weighed apo-PSS480/550 was prepared in DMSO in a 2 ml vial until the solid apo-PSS480 was fully dissolved. An equal volume of 4.2 mM zinc nitrate solution was then added. The resulting solution was placed in a water bath at 40°C and shaken frequently for 30 minutes to ensure complete complexation. A clear orange or red solution of 1 mM stock PSVue480/550 in 1:1 DMSO/water resulted. For staining, at least two samples of several stages (E10.5, E12.5, E14.5, E16.5, E18.5) were placed in stock solution diluted to 10μM in PBS and incubated at room temperature for 2 hours on a shaker. Samples were then washed several times with PBS and mounted in glycerol for imaging with a Leica TCS SP5 confocal. These procedures were performed on 4% PFA fixed tissue.

Plastic embedding/sectioning and Stevenel's Blue staining

One sample of wild type and CKO littermate were fixed in 2.5% glutaraldehyde overnight, washed several times with 0.1M phosphate buffer (pH 7.4), and then secondarily fixed in 2% osmium tetroxide (OsO_4) until myelinated fibers stained black. Following several washes in deionized water, the samples were then dehydrated through a graded ethanol series with a final incubation period in propylene oxide (PO). Finally, the samples were embedded in epoxy resin (Poly/Bed® 812 Embedding Media; Polyscieces, Inc.) and allowed to polymerize at 60°C for 24–48 hours. Sections were cut at 1μm on a Reichert-Jung Ultracut E microtome and stained with Stevenel's Blue made of 2% potassium permanganate and 1.3% methylene blue. Sections were mounted in DPX (Fluka) and imaged with a Nikon E800 microscope using Metamorph software for image processing.

Lipophilic dye tracing

The heads of three samples of E12.5, E14.5, E16.5 and E18.5 perfused wild type and CKO littermates were cut sagittally at the midline and lipophilic dye-soaked filter strips (Fritzsch *et al.*, 2005; Tonniges *et al.*, 2010) were inserted in rhombomere 4 to label the afferent and efferent fibers to the inner ear. Half heads were kept in 60°C oven for about 24 -72 hours (depending on the age) for diffusion of the dye from the brain to the ear. Then the ears were dissected, mounted in glycerol, coverslipped and imaged with a Leica TCS SP5 confocal microscope.

Bone and cartilage staining

One sample each of E16.5 and E18.5 old wild type and CKO littermates were fixed in 4% PFA and stained for bone and cartilage stain with minor modification as previously described (Ovchinnikov, 2009). Briefly, fixed neonate heads were isolated and tissue was carefully macerated using forceps. The resulting skulls were further fixed in 95% ethanol then transferred to acetone and incubated at room temperature overnight to remove fat. The skulls were immersed in alcian blue cartilage stain (0.01%) for to 24 hours, washed in 70% ethanol, then incubated in 1% potassium hydroxide at room temperature until the tissues were cleared. We counterstained for bone with alizarin red stain (0.005%) until a bones were sharply delineated. Finally, the samples were cleared in 1% potassium hydroxide/glycerol (1:1) for up to 2 days. Samples were submerged in glycerol and imaged with a Leica M205 FA microscope using LAS software for image processing.

Results

Macroscopic changes and the timeline of neurosensory loss

Foxg1-cre mediated conditional knockout (CKO) of *Dicer1* produced no obvious overall changes prior to E12.5 (Fig. 1A-A′). After E14.5, notable differences in skull morphology were the reduced growth of the eyes, snout and forebrain area, leading to a depression of the frontal bone anlage and a shortened distance between the eye and the ear (Fig. 1B–C′). The snout was markedly shortened and in older stages showed a reduced height. Overall the length of the head measured from the tip of the snout to the tentorium cerebelli was approximately 15% shorter. Most obvious was the shortening of the snout when compared with the lower jaw, which was almost as long as the snout in *Foxg1-cre::Dicer1* $^{f/f}$ mice (Fig. 1C, C′).

To investigate more closely the brain changes we cut the head into halves and scooped out the brains. Comparing the brains in both lateral and medial perspective showed no obvious differences until E12.5 when the forebrain showed accumulation of highly reflective cells. Such cells also appeared near the cerebellum and in various other places (Fig. 1D, 2A). By E14.5 the forebrain of the *Foxg1-cre* CKO mice was drastically reduced in size, formed only a small patch of white opaque cells compared to wild type littermates, and was completely gone by E18.5 (Fig. 1E–F, 2B-B′). At this late stage the forebrain consisted of only an empty space in the meninges anterior to the diencephalon (Fig. 1F, 2C). Further, there was also no olfactory bulb left (Fig. 2C). These data show that the entire forebrain (telencephalon) and the olfactory bulb start to develop normally but disappear within 6 days in *Foxg1-cre::Dicer1* $^{f/f}$ conditionalnull mutants.

An additional area of brain tissue loss was the cerebellum which was almost completely absent at E18.5 (Fig. 2F). The first obvious macroscopic indication of cerebellar change was around E14.5 when the cerebellum was more epithelial compared to the solid plate-like cerebellum of wild type littermates (Fig. 2E-E′). Closer examination of E12.5 showed opaque cells in high abundance in the cerebellum that was otherwise indistinguishable from

wildtypes (Fig. 2D-D′). Some minor reductions in other areas of the brain were negligible compared to the forebrain and cerebellar loss, and were always characterized by an accumulation of opaque cells (data not shown).

We next wanted to investigate in more detail the formation of bone in the heads of the *Foxg1-cre::Dicer1* $^{f/f}$ conditionalnull mutants using bone and cartilage staining. We expected that the absence of brain growth in the CKO mutant would result in premature closure of sutures. As predicted, the overall smaller skull of the CKO mice had narrower sutures between the forming bones of the skull (Fig. 3).

A prominent early change visible in the head of *Foxg1-cre::Dicer1* CKO mutant mice were changes in the eye. Around E12.5 the anterior part of the eye became depigmented and subsequently showed stunted growth (Fig. 1A, 4A) such that by E18.5 the *Foxg1-cre* CKO mutant eye was about the size of an E16.5 wild type eye. Direct comparison showed that at E18.5 the mutant eye was only the size of the wild type lens (Fig. 4C). In addition, the mutant eyes showed a pigment-free anterior streak, an asymmetric iris pointing toward the anterior half and had no lens beyond a few distributed cells inside the vitreous (Fig. 4C, E). The radius of the mutant eye was progressively lacking behind the wild type (Table 1). Assuming a spherical shape, this would result in an approximate 85% reduction in volume of the mutant eye at E18.5 (Table 1). There was no lens in these eyes and a small protrusion extended from the neural retina to partially covering the lens space (Fig. 4E). While a retina was obviously present, the cellular layers so characteristic of the normal littermate retina could not be distinguished (Fig. 4D-D′, E-E″). We tentatively identified a ganglion cell layer with little indication of nerve fibers and a partially developed inner plexiform layer. The anterior half of the retina was even more disorganized than the posterior retina, showing rosettes and overgrowth of receptor anlage (Fig. 4E″).

As with the eyes, the changes in the ear started around E12.5 with the appearance of opaque cells in the delaminated sensory neurons. A reduction in size of the ear was first apparent at E14.5. Formation of periotic cartilage in later stages indicated that the size of the otocyst of CKO mutant mice was reduced at E18.5, but also showed less ossification of the ear and a smaller tympanic ring (Fig. 5A, A). Interestingly the inner ear had only a superior part left with a short ventral extension reminiscent of the cochlear duct (Fig. 5B). Small otoconia were usually present near the small posteroventral duct, as well as within this small duct (Fig. 5B). This indicates that possibly a gravistatic sensory epithelium might have formed in the ear. We investigated neurosensory development of the *Foxg1-cre* CKO mutant ear using anti-β tubulin and anti-Myo7a immunochemistry to label neurons and hair cells, respectively (Fig. 5H–J). Our data indicated the presence of very few nerve fibers to a small patch of hair cells resembling in shape and position of the utricle. In addition, a few Myo7a-positive cells with a single fiber innervating them were found in the small posterior duct. We tentatively identify these cells as the ‘saccule’ as they are reminiscent of the reduced saccule of *Pax2-cre::Dicer1* $^{f/f}$ mice (Soukup *et al.*, 2009). It is unclear if larger prosensory domains characterized by expression of specific genes form initially and degenerate or if they never develop, as pigment cells usually identified with such domains, manage to reach the reduced ear but remain in the otocyst wall. We next investigated the development of innervations. Some innervation to the ear develops initially but ultimately was reduced to a few remaining fibers to vestibular endorgans only (Fig. 5D–G).

Because of the apparent reduction in size of the snout by approximately 10% in all dimensions we also investigated the olfactory system. Olfactory receptors seem to develop initially and project to forebrain (Fig. 2A; insert). However, at E18.5 we found a reduction of conchae and loss presumably of all olfactory neurons (data not shown), defects that are more profound than those reported in *Foxg1* null mice (Duggan *et al.*, 2008;Kawauchi *et al.*,

2009). No olfactory fibers could be detected passing through the cribrifom plate, which was solid bone. The inability to innervate the absent olfactory bulb (Fig. 1C, 2C) could certainly accelerate the demise of olfactory receptors, but it is unclear where and when loss started.

In summary, loss of *Foxg1-cre* mediated *Dicer1* results in complete loss of certain areas of the brain (forebrain, olfactory bulb, and cerebellum) near complete loss of the inner ear, reduction of the eye and of conchae as well as olfactory epithelium. We next wanted to investigate how this loss was orchestrated at the molecular level in the absence of Dicer1 enzyme and likely all miRNAs and other small RNAs.

Loss of cells follows Cre expression which is followed by loss of miRNA, upregulation of anti-cleaved Caspase 3 and digestion of dying cells by macrophages—We first investigated the upregulation of *cre* using immunocytochemistry and found *cre* expression in the forebrain, cerebellum and ear as early as E12.5 (Fig. 2D′; insert) consistent with the known expression of *Foxg1*. We next investigated the expression of one miRNA as a proxy for other neuronal miRNAs, miR-124. Expression of this miRNA were detected in the forebrain (data not shown) and the ear at E11.5 (Fig. 6A, B), but disappeared in the ear, the forebrain and the cerebellum around E12.5 (Fig. 6C, D). Areas without miR-124 were abundant throughout the brain around E14.5 and no miR-124 was visible in the olfactory epithelium past E14.5 (data not shown). These data suggest that it takes approximately 6 days after the *cre* mediated deletion of *Dicer1* before the miRs are almost completely depleted.

Following our previous data (Soukup *et al.*, 2009) and those of others (Huang *et al.*, 2010; Shi *et al.*, 2010), we expect that the miRNA depletion will result in apoptosis of proliferating and differentiating neuronal precursors. We therefore next investigated the distribution of apoptotic cells using anti-cleaved caspase 3 antibodies and a PSVue stain that targets phosphatidylserine (PS) exposed on the membranes of dying cells (MTTI). Phosphatidylserine is normally found only in the inner plasma membrane leaflet of membranes and is inaccessible to this stain. Flippases normally transfer any PS that diffuses into the outer leaflet back into the inner leaflet. However, these flippases are the target of caspase 7 which in turn is activated by caspase 3. Flippases are inactivated when caspase 3/7 are activated in apoptotic cells. Without flippases, PS accumulates in the outer leaflet (Krijnen *et al.*, 2010). Exposure of phosphatidylserine in the outer leaflet is a signal to macrophages to engulf apoptotic cells. The PSVue dye was designed for labeling these late-stage dying cells. In addition we used anti-β tubulin to stain developed neurons to understand if neurons start to differentiate and subsequently die or die shortly after cell cycle exit without any differentiation.

Eyes and ears—While loss of the forebrain, olfactory bulb and cerebellum was complete at E18.5 (Figs. 1, 2), loss of eyes and ears was incomplete but possibly for different reasons. *Foxg1* is only expressed in the anterior half of the retina whereas the posterior half expresses a different forkhead gene, *Foxd1* (Herrera *et al.*, 2004). Consequently there is no *Foxg1-cre* expression in the posterior retina and we find little defects (Fig. 4). In contrast, the anterior retina seems to degenerate completely. Near equatorial sections through the retina show that the posterior retina begins differentiation at E18.5 whereas the anterior retina shows numerous condensed nuclei (Fig. 4E). It remains unclear how and why the lens disintegrates in these eyes but it is definitely absent by E18.5 (Fig. 4E). These data suggest that the anterior half of the eye may completely disappear by CKO induced cell death. The remaining posterior half reforms the eye cup but is unable to restore the full growth of the eye, leading to a markedly smaller and deformed eye (Fig. 1, 4; Table 1).

Previous work has demonstrated that only very few areas of the developing ear are free of *Foxg1* such as the stria vascularis (Pauley *et al.*, 2006), an area of the lateral wall of the cochlea specialized in the secretion of the potassium-rich endolymph. In particular all neurosensory cells seem to be highly positive for *Foxg1,* suggesting that perhaps all neurosensory precursors express *Foxg1* (Hwang *et al.*, 2009; Pauley *et al.*, 2006). Consistent with this expectation, we found at E18.5 a near complete loss of all neurosensory cells and a near complete loss of the entire ear with an elongated vesicle remaining (Fig. 5B). Only one patch of hair cells remained that expressed myosin 7a, a marker for hair cells. Based on its position near the undifferentiated canal growth plate (Fig. 5B, H–J) and due to its kidney shape, it is likely the utricle but could be a fusion of some epithelia (Nichols *et al.*, 2008). Interestingly, a short ventral duct was always present in these mutants that had a few Myo7a positive hair cells near the single primary epithelium in the vestibular sac. This extension appears in shape like a shortened cochlear duct. Innervation to this truncated ear was by several fibers to the major sensory epithelium whereas a single fiber extended to the few cells in the base of the cochlear duct.

This near complete loss of the ear could come about through spatial sparing of some cells or through delayed loss. We therefore next investigated the state of differentiation of the neurosensory system in earlier embryos. Interestingly, many more nerve fibers were detected radiating to multiple areas of the ear consistent with posterior canal crista, cochlea, etc (Fig. 5D–G). However, this early extension of nerve fibers soon disappeared resulting in the limited innervation that remained at E18.5 (Fig. 5F, G, I, J). We therefore suggest that many neurons are lost with a delay because of delayed loss of *Dicer1* and miRNAs. Once both have disappeared, the partially differentiated neurons that extend processes will die. We directly investigated this hypothesis using anti-caspase 3 staining in combination with PSVue staining and found degenerating neurons in the ganglion (Fig. 6E, E′, F, F′). These data suggest that neurosensory cells in the ear are as dependent for their differentiation on miRNAs as are neurons in the CNS and undergo a very similar cell death of partially differentiated neurons followed by phagocytosis through macrophages/activated microglia. *In situ* hybridization using miR-124 showed absence of this miR as early as E12.5 (Fig. 6C, D), but it cannot be excluded that other miRNAs might remain longer in some neurons, thus enabling some limited development. Whether the very few neurons and Myo7a-positive hair cells we found at E18.5 will remain after birth could not be tested due to perinatal lethality of the mutant embryos. Based on the uniform later fate of all cells in the forebrain (see below), we assume that differentiating cells that go on to survive the longest have for whatever reason managed to retain enough miRNAs to initiate that process but eventually are depleted like other cells and undergo apoptosis.

Forebrain and cerebellum—Consistent with this scenario was that numerous anti-cleaved caspase 3 and PSVue-positive cells were present in the forebrain at E12.5 (Fig. 7), and by E14.5 the forebrain was reduced to a small vesicle attached to the lateral wall of the diencephalon with very high levels of reflective cells (Fig. 1E, 2B). By E18.5 not even a trace of a forebrain remained (Fig. 1F, 2C), clearly indicating that all developing neurons critically depend on *Dicer1*-mediated replenishment of small RNAs for survival. Within the forebrain, cell death started in the future cortical areas, consistent with the upregulation of *Foxg1* (Tao and Lai, 1992). At E12.5 the entire forebrain was filled with macrophages containing multiple lumps of cellular debris that stain positive for PSVue. Counterstaining with anti-β tubulin shows multiple neuronal processes associated with anti-caspase 3 positive cells but not with PSVue-stained cells inside macrophages. These data show that at least some neurons start their differentiation. Notably, olfactory axons reach into the forebrain at this stage but interact only with anti-caspase 3 positive cells (Fig. 7). Later stages show the near complete loss of tubulin and caspase 3 with most cells forming debris inside macrophages that still stain positive for phosphatidylserine (data not shown). It

remains unclear for a given neuron how onset of differentiation relates to complete depletion of all miRNA.

A similar sequence of events was found for the cerebellum but with a slight delay in onset and a faster completion of loss. At E12.5 the cerebellar anlage already showed many anti-cleaved caspase3 positive degenerating cells but comparatively fewer anti-phosphatidylserine positive cells inside macrophages (Fig. 8A, B). By E14.5 the cerebellum was already massively reduced with the future vermis being completely eliminated and the future hemispheres being filled with numerous macrophages filled with cellular debris (Fig. 2E). By E18.5 there was no cerebellum, and the choroid plexus (CP) of the IVth ventricle was attached directly onto the midbrain (Fig. 2F). These data show a fast upregulation of critical steps in apoptosis followed by macrophage-mediated resorption of the debris (Fig. 8A-B″) in all brain areas with uniform expression of *Foxg1-cre*.

In summary, eyes and ears follow in principle the same rapid degeneration process in the absence of *Dicer1* as do neurons in the CNS. However, there is incomplete loss of the retina due to expression of *Foxg1-cre* only in the anterior half of the eye. The limited number of hair cells and the few neurons remaining in the E18.5 ear could reflect a transient retention or might indicate that at least some hair cells can form in the absence of miRNAs, possibly correlated with less *Foxg1-cre* expression or very early development and thus more advanced stages in development before *Dicer1* and miRNAs were depleted. Birthdating these cells using BrdU could test this hypothesis. Clearly, brain areas with uniform, early expression of *Foxg1* disappear entirely (forebrain), but loss is also surprisingly profound in areas with little known *Foxg1* expression (cerebellum).

Discussion

The purpose of our investigation was to establish a mouse model that eliminates all major cranial sensory organs as well as the two most enlarged mammalian brain areas, the forebrain and the cerebellum, to investigate the effect of loss of these building blocks of the head on the craniofacial development. Using *Foxg1-cre* to eliminate the lead enzyme that generates active miRNAs, Dicer1, we succeeded in entirely eliminating the forebrain and the cerebellum, and the anterior half of the eye. We also almost entirely abolished inner ear development which in turn resulted in a truncated development of the otic capsule. The olfactory sensory epithelium and the olfactory bulb were also absent. Despite this significant loss or downsizing effect of our conditional deletion of *Dicer1*, we had only comparatively minor changes in the craniofacial development mostly associated with the loss of olfactory epithelium and forebrain. These data suggest that the new head idea, arguing that the formation of neural crest and placode associated sensory organs are major aspects to the craniate head (Gans and Northcutt, 1983) cannot be easily tested through embryonic reduction of the craniate sensory organs and major parts of the mammalian brain at the latest stage possible with our approach. Obviously, even transient formation of these structures suffices to interact with the surrounding mesenchyme to start the formation of the skull, olfactory and otic capsule and thus a surprisingly normal head. Consistent with this interpretation are recent data obtained with a similar approach using *Wnt1-cre* to eliminate floxed *Dicer1* in neural crest. This early depletion of *Dicer1* results in the elimination of all neural crest derived tissue and profound cranio-facial malformations (Huang *et al.*, 2010). Therefore, timing the depletion of *Dicer1* to an earlier stage, thus blocking initial formation of these sensory and brain anlage could yield a more profound effect on cranio-facial development. Alternatively, deletion of all cells at even earlier stages using inducible expression of diphtheria toxin (Okuyama *et al.*, 2010) should result in more profound effects on cranio-facial development.

Previous work has identified certain miRNAs as extremely conserved (Pierce *et al.*, 2008) with miR-124 being among the very few that shows not even a single nucleotide variation among animals (Peterson *et al.*, 2009). It has been suggested that such extreme conservation indicates extreme conservation for an essential function completed by such a conserved gene. If so, presence of miR-124 could be necessary for normal neuronal development. Consistent with several previous data showing a rapid loss of neurons after miRNAs are eliminated (Hebert *et al.*, 2010; Huang *et al.*, 2010; Shi *et al.*, 2010), we show here that all forebrain, olfactory bulb, cerebellar neurons and neurosensory cells of the ear undergo a rapid degeneration within a few days after miR-124 is depleted following the conditional deletion of *Dicer1* with *Foxg1-cre*. These data support the notion that in particular neuronal development is crucially dependent on small RNAs. Like *Pax2*, *Foxg1* is also expressed in non-neural tissue such as the naso-pharyngeal duct and the larynx. We could not detect any noticeable alterations in these structures, suggesting that miRNA-mediated differentiation is more essential for neurons and sensory cells than for non-sensory cells.

In all tissues examined there is a progression of loss of the indicator miRNAs tested here which is followed in turn by a delayed upregulation of anti-cleaved caspase 3, followed by the appearance of phosphatidylserine on the surface of dying cells (Fig. 6–8). Engulfment of the dying neurons by macrophages seems to be triggered quickly after phospatidylserine appears on the surface of effected cells as few were found to be positive for PSVue but not yet aggregated in a macrophage. In contrast, anti-cleaved caspase 3 was mostly in single cells but could also be detected inside macrophages, rarely co-expressed with phasphatidylserine stained by PSVue (Fig. 8). This process appears to be similar in the PNS or the CNS with the only difference being that in the PNS the activated microglia cells are replaced by macrophages. More recent data suggest that miRNA depletion leads to altered tau phosphorylation which in turn might relate to neuronal degeneration in the absence of miRNAs in various neurodegenerative diseases such as Alzeimers disease (Hebert *et al.*, 2010) as well as in aging (Chen *et al.*, 2010).

Why a small number of hair cells survives into late embryonic stages and receives a very small innervation remains unclear. However, we found a similar pattern of remaining hair cells and innervation in same staged embryos from several litters, implying that the pattern of remaining hair cells and innervating neurons suggests a specific ability to sidestep the effect of Dicer1 enzyme depletion. If this comes about through delayed expression of *Foxg1-cre* in these cells or their ability to maintain longer at least some miRNA remains to be seen. Despite absence of an indicator miRNA, we cannot exclude that others not yet characterized in their expression as being unique to hair cells and neurons may exist and may show a different profile of loss after depletion of *Dicer1*. Alternatively, vertebrate hair cells have been suggested to be related to somewhat similar cells found in jellyfish (Fritzsch *et al.*, 2007). Jellyfish have no known miRNA (Peterson *et al.*, 2009). It is therefore possible that some hair cell formation can occur in the complete absence of miRNA, reverting to non-miRNA mediated development.

The data concerning a massive loss of neuronal and sensory cells in areas of *Foxg1-cre* expression are clear-cut, but there are two notable exceptions suggesting non-neuronal tissue loss, the non-sensory epithelium of the ear and the placode derived lens. A lens may form initially but seems to degenerate with an approximately identical time course of the retina degeneration. The lens is, like other placodally derived tissue, carved out of the preplacode that surrounds the brain anlage (Streit, 2007). This region is positive for genes now known to be important for neurosensory development such as *Eya1* (Zou *et al.*, 2004) and *Pax 2/8* [ear, (Bouchard *et al.*, 2010)] or *Pax6* [lens and eye (Bailey *et al.*, 2006)]. It is possible that the lens has a near neuronal status in development and requires as much miRNA for its

development as do neurons. Undoubtedly, the lens has disappeared at E18.5 and this may come about by degeneration analogous to the neuronal degeneration we report here.

In the ear, it is possible that the loss of prosensory areas stunts growth as those areas are implied in directing growth of non-sensory structures such as the canals which clearly are stunted at the level of the canal plate as in *Fgf10* null mice that also eliminate the canal cristae (Pauley *et al.*, 2003). Alternatively, as with the lens, the loss of most non-neural tissue in the ear may relate to the same placodal origin issues as it was shown that many otic placodal markers are expressed overlapping throughout the otic placode, only to segregate from non-neuronal tissue in the course of ear development (Zou *et al.*, 2008).

Recent data suggested that growth of the skull is directly proportional to the growth of the brain in mammals, including humans (Gibbons, 2010). Our data suggest that absence of forebrain relates to a smaller suture between the growing plates of the bones (Fig. 3), possibly resulting in a reduced skull size, if the mice would survive.

In conclusion, we analyzed the effects of a *Foxg1-cre*-mediated conditional deletion of Dicer1, the enzyme that processes miRNAs to their active states, on the brains and cranial sensory systems of mice. We found that Dicer1 enzyme is necessary for proper forebrain, eye, ear, and cerebellum development. We establish that neuronal development is critically dependent upon miRNA function and absence of all small RNAs leads to complete loss of neurons within a few days. In support of this suggestion, we provide direct evidence that the activation of caspase 3 and appearance of phosphatidylserine in the outer leaflet of cells is correlated with disappearance of miRNAs in partially differentiating neurons. Our data suggest that the effects of the conditional deletion of *Dicer1* are most profound in neuronal cells but may also affect non-neuronal placode derived tissue, possibly due to the neuron-like status of placodal tissue. Our data confirm and extend recent observations using other *cre* drivers on developing neurosensory systems (Huang *et al.*, 2010; Soukup *et al.*, 2009).

Acknowledgments

This work was supported by the NIDCD (R01 DC 005590 to BF; DC009025 to GAS). We thank Drs. Harfe and Hebert for making the floxed *Dicer1* and the *Foxg1-cre* lines available. We thank MTTI research, in particular Brian Gray for making the PSVue dyes available to us. The Leica TCS SP5 confocal microscope was purchased in part with a grant from the Roy J. Carver Foundation. We thank the University of Iowa Central Microscopy Research Facility (CMRF) for the use of the SEM and the Office of the Vice President for Research (OVPR), CLAS, and the P30 core grant for support. Finally, we would like to thank Christopher Donahue for his skilled technical assistance.

References

Bailey AP, Bhattacharyya S, Bronner-Fraser M, Streit A. Lens specification is the ground state of all sensory placodes, from which FGF promotes olfactory identity. Dev Cell. 2006; 11:505–517. [PubMed: 17011490]

Bouchard M, de Caprona D, Busslinger M, Xu P, Fritzsch B. Pax2 and Pax8 cooperate in mouse inner ear morphogenesis and innervation. BMC Dev Biol. 2010; 10:89. [PubMed: 20727173]

Chen LH, Chiou GY, Chen YW, Li HY, Chiou SH. microRNA and aging: a novel modulator in regulating the aging network. Ageing Res Rev. 2010; 9(Suppl 1):S59–66. [PubMed: 20708718]

Clevidence DE, Overdier DG, Tao W, Qian X, Pani L, Lai E, Costa RH. Identification of nine tissue-specific transcription factors of the hepatocyte nuclear factor 3/forkhead DNA-binding-domain family. Proc Natl Acad Sci U S A. 1993; 90:3948–3952. [PubMed: 7683413]

Duggan CD, DeMaria S, Baudhuin A, Stafford D, Ngai J. Foxg1 is required for development of the vertebrate olfactory system. J Neurosci. 2008; 28:5229–5239. [PubMed: 18480279]

Fritzsch B, Beisel KW, Pauley S, Soukup G. Molecular evolution of the vertebrate mechanosensory cell and ear. Int J Dev Biol. 2007; 51:663–678. [PubMed: 17891725]

Fritzsch, B.; Glover, JC. Evolution of the deuterostome central nervous system: an intercalation of developmental patterning processes with cellular specification processes. In: Kaas, JH., editor. Evolution of the Nervous System. Oxford: Academic Press; 2006. p. 1-24.

Fritzsch B, Muirhead KA, Feng F, Gray BD, Ohlsson-Wilhelm BM. Diffusion and imaging properties of three new lipophilic tracers, NeuroVue Maroon, NeuroVue Red and NeuroVue Green and their use for double and triple labeling of neuronal profile. Brain Res Bull. 2005; 66:249–258. [PubMed: 16023922]

Gans C, Northcutt RG. Neural crest and the origin of vertebrates: a new head. Science. 1983; 220:268–273. [PubMed: 17732898]

Gibbons A. Paleoanthropology. Neandertal brain growth shows a head start for moderns. Science. 2010; 330:900–901. [PubMed: 21071640]

Hanashima C, Li SC, Shen L, Lai E, Fishell G. Foxg1 suppresses early cortical cell fate. Science. 2004; 303:56–59. [PubMed: 14704420]

Hanashima C, Shen L, Li SC, Lai E. Brain factor-1 controls the proliferation and differentiation of neocortical progenitor cells through independent mechanisms. J Neurosci. 2002; 22:6526–6536. [PubMed: 12151532]

Hatini V, Tao W, Lai E. Expression of winged helix genes, BF-1 and BF-2, define adjacent domains within the developing forebrain and retina. J Neurobiol. 1994; 25:1293–1309. [PubMed: 7815060]

Hebert JM, McConnell SK. Targeting of cre to the Foxg1 (BF-1) locus mediates loxP recombination in the telencephalon and other developing head structures. Dev Biol. 2000; 222:296–306. [PubMed: 10837119]

Hebert SS, Papadopoulou AS, Smith P, Galas MC, Planel E, Silahtaroglu AN, Sergeant N, Buee L, De Strooper B. Genetic ablation of Dicer in adult forebrain neurons results in abnormal tau hyperphosphorylation and neurodegeneration. Hum Mol Genet. 2010; 19:3959–3969. [PubMed: 20660113]

Herrera E, Marcus R, Li S, Williams SE, Erskine L, Lai E, Mason C. Foxd1 is required for proper formation of the optic chiasm. Development. 2004; 131:5727–5739. [PubMed: 15509772]

Huang T, Liu Y, Huang M, Zhao X, Cheng L. Wnt1-cre-mediated conditional loss of Dicer results in malformation of the midbrain and cerebellum and failure of neural crest and dopaminergic differentiation in mice. J Mol Cell Biol. 2010; 2:152–163. [PubMed: 20457670]

Hwang CH, Simeone A, Lai E, Wu DK. Foxg1 is required for proper separation and formation of sensory cristae during inner ear development. Dev Dyn. 2009; 238:2725–2734. [PubMed: 19842177]

Jahan I, Pan N, Kersigo J, Fritzsch B. Neurod1 suppresses hair cell differentiation in ear ganglia and regulates hair cell subtype development in the cochlea. PLoS One. 2010; 5:e11661. [PubMed: 20661473]

Kawauchi S, Kim J, Santos R, Wu HH, Lander AD, Calof AL. Foxg1 promotes olfactory neurogenesis by antagonizing Gdf11. Development. 2009; 136:1453–1464. [PubMed: 19297409]

Krijnen PA, Sipkens JA, Molling JW, Rauwerda JA, Stehouwer CD, Muller A, Paulus WJ, van Nieuw Amerongen GP, Hack CE, Verhoeven AJ, van Hinsbergh VW, Niessen HW. Inhibition of Rho-ROCK signaling induces apoptotic and non-apoptotic PS exposure in cardiomyocytes via inhibition of flippase. J Mol Cell Cardiol. 2010; 49:781–790. [PubMed: 20691698]

Nichols DH, Pauley S, Jahan I, Beisel KW, Millen KJ, Fritzsch B. Lmx1a is required for segregation of sensory epithelia and normal ear histogenesis and morphogenesis. Cell Tissue Res. 2008; 334:339–358. [PubMed: 18985389]

Nieuwenhuys R. Deuterostome brains: synopsis and commentary. Brain Res Bull. 2002; 57:257–270. [PubMed: 11922969]

Nieuwenhuys, R.; Donkelaar, HJt; Nicholson, C. The central nervous system of vertebrates. Vol. 3. Berlin; New York: Springer; 1998. p. xvip. 2219

Ohyama T, Groves AK. Generation of Pax2-Cre mice by modification of a Pax2 bacterial artificial chromosome. Genesis. 2004; 38:195–199. [PubMed: 15083520]

Okuyama M, Kayama H, Atarashi K, Saiga H, Kimura T, Waisman A, Yamamoto M, Takeda K. A novel in vivo inducible dendritic cell ablation model in mice. Biochem Biophys Res Commun. 2010

Ovchinnikov, D. Cold Spring Harb Protoc. Vol. 2009. 2009. Alcian blue/alizarin red staining of cartilage and bone in mouse. pdb prot5170

Pauley S, Lai E, Fritzsch B. Foxg1 is required for morphogenesis and histogenesis of the mammalian inner ear. Dev Dyn. 2006; 235:2470–2482. [PubMed: 16691564]

Pauley S, Wright TJ, Pirvola U, Ornitz D, Beisel K, Fritzsch B. Expression and function of FGF10 in mammalian inner ear development. Dev Dyn. 2003; 227:203–215. [PubMed: 12761848]

Peterson KJ, Dietrich MR, McPeek MA. MicroRNAs and metazoan macroevolution: insights into canalization, complexity, and the Cambrian explosion. Bioessays. 2009; 31:736–747. [PubMed: 19472371]

Pierce ML, Weston MD, Fritzsch B, Gabel HW, Ruvkun G, Soukup GA. MicroRNA-183 family conservation and ciliated neurosensory organ expression. Evol Dev. 2008; 10:106–113. [PubMed: 18184361]

Shi Y, Zhao X, Hsieh J, Wichterle H, Impey S, Banerjee S, Neveu P, Kosik KS. MicroRNA regulation of neural stem cells and neurogenesis. J Neurosci. 2010; 30:14931–14936. [PubMed: 21068294]

Soukup GA, Fritzsch B, Pierce ML, Weston MD, Jahan I, McManus MT, Harfe BD. Residual microRNA expression dictates the extent of inner ear development in conditional Dicer knockout mice. Dev Biol. 2009; 328:328–341. [PubMed: 19389351]

Streit A. The preplacodal region: an ectodermal domain with multipotential progenitors that contribute to sense organs and cranial sensory ganglia. Int J Dev Biol. 2007; 51:447–461. [PubMed: 17891708]

Tao W, Lai E. Telencephalon-restricted expression of BF-1, a new member of the HNF-3/fork head gene family, in the developing rat brain. Neuron. 1992; 8:957–966. [PubMed: 1350202]

Tonniges J, Hansen M, Duncan J, Bassett MJ, Fritzsch B, Gray BD, Easwaran A, Nichols MG. Photo- and bio-physical characterization of novel violet and near-infrared lipophilic fluorophores for neuronal tracing. J Microsc. 2010; 239:117–134. [PubMed: 20629917]

Xuan S, Baptista CA, Balas G, Tao W, Soares VC, Lai E. Winged helix transcription factor BF-1 is essential for the development of the cerebral hemispheres. Neuron. 1995; 14:1141–1152. [PubMed: 7605629]

Young NM, Chong HJ, Hu D, Hallgrimsson B, Marcucio RS. Quantitative analyses link modulation of sonic hedgehog signaling to continuous variation in facial growth and shape. Development. 2010; 137:3405–3409. [PubMed: 20826528]

Zou D, Erickson C, Kim EH, Jin D, Fritzsch B, Xu PX. Eya1 gene dosage critically affects the development of sensory epitheliain the mammalian inner ear. Hum Mol Genet. 2008; 17:3340–3356. [PubMed: 18678597]

Zou D, Silvius D, Fritzsch B, Xu PX. Eya1 and Six1 are essential for early steps of sensory neurogenesis in mammalian cranial placodes. Development. 2004; 131:5561–5572. [PubMed: 15496442]

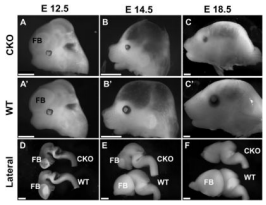

Fig. 1.

These images show the progressive change in the appearance of the head of wild type (WT) and *Foxg1-cre::Dicer1*$^{f/f}$ (CKO) mice. Note the limited reduction in the forebrain (FB) in the CKO mice at E12.5 (A, A′, D), suggesting that the initial formation of the forebrain is normal. Marked changes are obvious by E14.5 with a severe reduction of the forebrain, shortening of the skull and a reduction in eye size (B, B′, E). By E18.5 neither the forebrain nor olfactory bulb are present and the eye is much smaller in CKO mice (C, C′, F). The skull develops a sunken-in appearance and the snout is reduced in all dimensions by approximately 10%. Bar indicates 1 cm (A–C) and 0.5 mm (D–F).

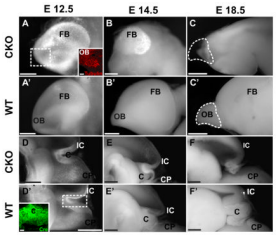

Fig. 2.

Detailed examination of the brain shows not only the dramatic reduction in size and loss of the forebrain (A–C) but also the complete loss of the cerebellum (D–F) and olfactory bulb (C-C′) in the *Foxg1-cre::Dicer1*$^{f/f}$ (CKO) mice. Note the increasing density of many opaque cells in the degenerating forebrain (A, B) and cerebellum (D, E). While the forebrain and cerebellum of the CKO are almost identical to the WT at E12.5 (A-A′, D-D′) size reductions are apparent at E14.5 (B-B′, E-E′), and loss of both areas is obvious at E18.5 (C-C′, F-F′). Note that the loss of the cerebellum shows normal early embryonic development (D, D′) followed by complete loss (F, F′). Anti-cre immunochemistry of the WT cerebellum (*Foxg1-cre::Dicer1*$^{f/+}$) reveals high positivity at E12.5 (D′ insert). Anti-β tubulin immunochemistry on the E12.5 CKO brain reveals positive fibers in the area of the olfactory bulb indicating the normal initial formation of olfactory neuron projection (insert in A). By E18.5 only vacant meninges remain where the olfactory bulb started to develop (C, C′). FB, forebrain; IC, inferior colliculus; C, cerebellum; CP, choroid plexus; OB, olfactory bulb. Bar indicates 2mm bars in C, C′ and F, F′, 100μm A and D′ insert, and 1mm other images.

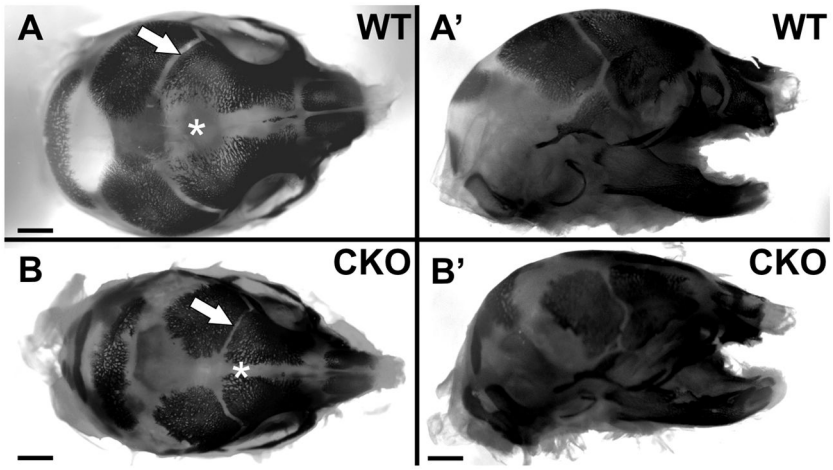

Fig. 3.

Staining with Alizarin red S for bone reveals that ossification has smaller sutures between the growing bony plates of the skull in *Foxg1-cre::Dicer1*$^{f/f}$ (CKO) mice (arrow and asterisk in A, B). The overall reduction of the frontal bone growth and smaller eye socket are obvious in the lateral view. Bar indicates 1 mm.

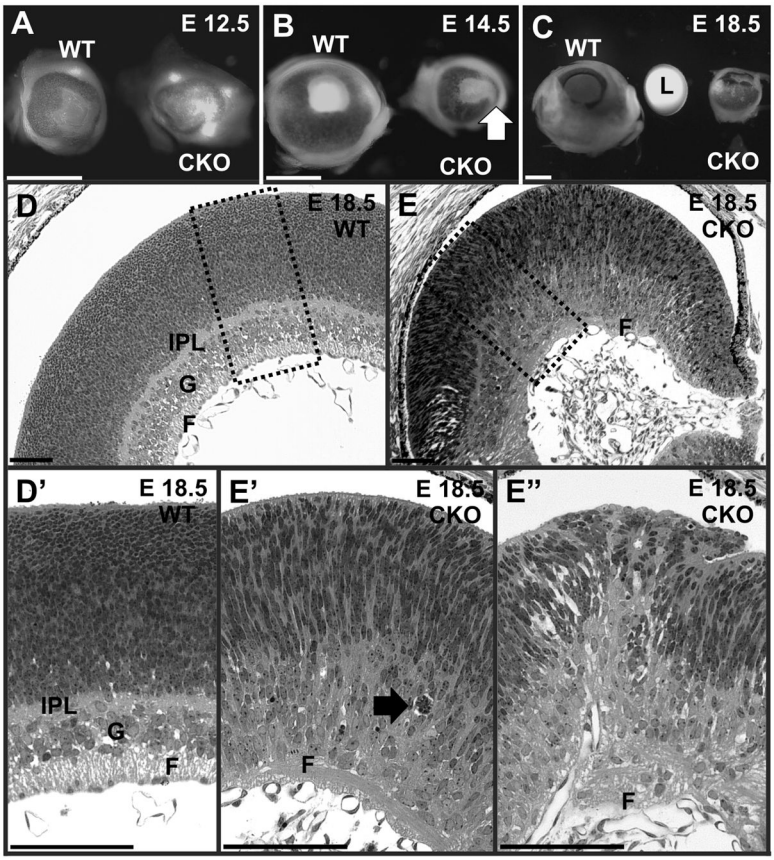

Fig. 4.

Eyes of wild type (WT) and *Foxg1-cre::Dicer1*$^{f/f}$ (CKO) mice start development almost identical but show differences in growth over the observed period. The eyes of CKO mice show almost no growth past E12.5 whereas there is doubling in the diameter and a 20x increase in the volume (see Table 1) in the WT animal. The anterior (right) part of the CKO eye shows a reduced size and loss of pigment at E14.5 (B, arrow), suggesting a loss of the anterior, *Foxg1-Cre* expressing part of the eye. At E18.5 the reduced eye of the CKO is approximately the same size of the lens of the WT animal (C). In addition, histology does not reveal a lens in the E18.5 CKO eye but instead shows a protrusion of the neural retina to fill the gap (E). Beyond the size differences are histological differences. The control retina showed well developed fiber (F), ganglion (G) and inner plexiform layers (IPL) but no such layers are as obvious in the CKO mice (D, E). Higher magnification shows the presence of apoptotic cells as single profiles or several of them engulfed by a macrophage-like cell (arrow in E). F, fiber layer; G, ganglion cell layer; IPL, inner plexiform layer; L, lens. Bar indicates 1mm A–C and 100μm D–E″.

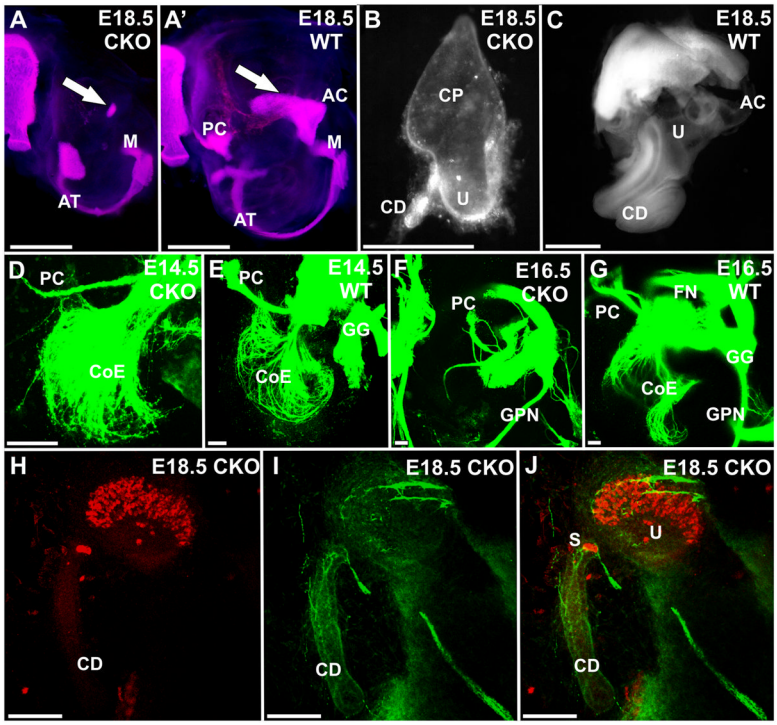

Fig. 5.

The otic capsule of *Foxg1-cre::Dicer1*$^{f/f}$ (CKO) mice is modestly reduced at E18.5 (A) and shows a nearly complete absence of ossification of the otic capsule. Cartilage and bone staining (A, A′) indicates that ossification of the maleus (M) seems to proceed normally and a smaller annulus tympanicum (AT) forms that undergoes normal ossification. In contrast, the inner ear is reduced by 38.6 % (note differences in magnification in B, C). The CKO inner ear shows loss of canal formation beyond the canal plate found at E12.5, and has a very short cochlear duct (CD) instead of a coiled cochlea (B, C). Labeling of afferents and efferents to the ear with lipophilic dyes inserted into the brainstem shows that fibers grow out nearly normal up to E14.5 (D, E) but are much reduced at E16.5 (F, G). Notably is the near complete loss of fiber growth to the cochlea (F) and the reduction to vestibular organs such as the posterior canal crista (PC). Fibers outside the ear such as the facial nerve (FN), geniculate ganglion (GG) and greater petrosal nerve (GPN) are near normal (F, G). Tracing the development of hair cells with Myo7a (H, J) and anti-β tubulin immunochemistry (I, J) reveals hair cells only in a single organ, tentatively identified as the utricle (H, J), and 2–3 cells at the base of the cochlear duct, possibly representing the saccule (S). Nerve fibers reach these hair cells and a few very thin, likely autonomic fibers are found around the cochlear duct. AC, anterior canal crista; CD, cochlear duct; CP, canal plate; PC, posterior canal crista; S, saccule; U, utricle; CoE, cochlear efferents; FN, facial nerve; GG, geniculate ganglion; GPN, greater petrosal nerve. Bar indicates 1mm A–C and 100 um D–J.

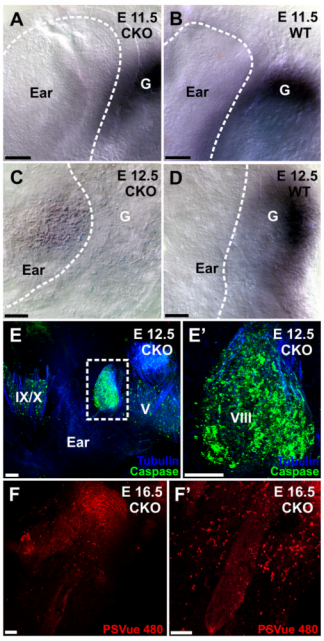

Fig. 6.

In situ hybridization using a LNA probe for miR-124 shows little difference at E11.5 (A, B), indicating that sensory neurons form a ganglion (G) and produce functional miRNA. In contrast, by E12.5 there is no miR-124 left in the ganglion of the *Foxg1-cre::Dicer1*$^{f/f}$ CKO (C) whereas the control littermate reacted with the CKO ear shows prominent staining (D). Staining for anti-cleaved caspase 3 at E12.5 shows prominent expression in the inner ear ganglion but much reduced presence of cleaved caspase 3 in the adjacent trigeminal (V) and glossopharyngeal/vagal (IX, X) ganglia (E). Higher power shows the nearly ubiquitous presence of anti-cleaved caspase 3 expressing cells that nevertheless show some anti-β tubulin staining (blue, E-E′), indicating some neuronal development. Staining for PSVue (F, F′) shows many cells staining positive throughout the ear at E16.5, indicating continued cell degeneration during later development. Bar indicates 100 μm.

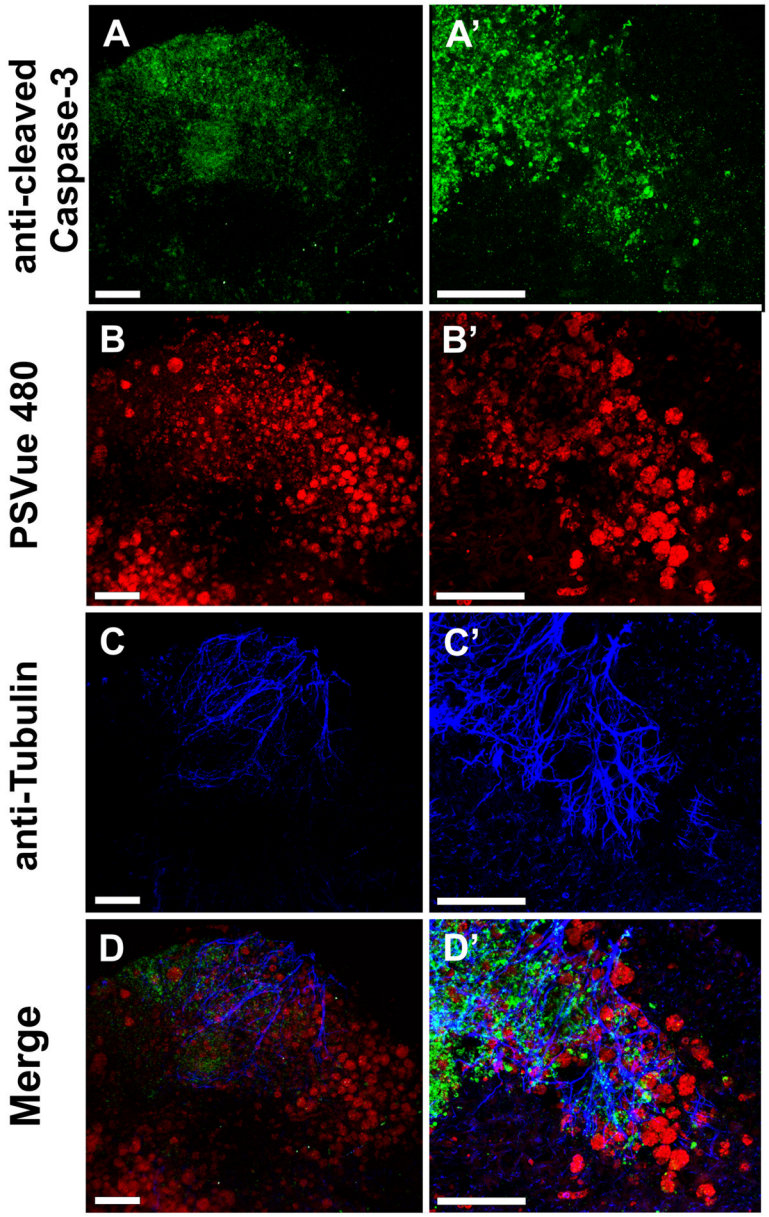

Fig. 7.

Immunochemistry of a *Foxg1-cre::Dicer1*$^{f/f}$ CKO reveals numerous anti-cleaved caspase 3 positive cells in the forebrain at E12.5 (A, A′). These anti-cleaved caspase 3 positive cells form a gradient with the highest concentration near the rostral (top) pole of the forebrain. Higher power images (A′) indicate that nearly every cell in the most rostral area shows anti-caspase 3 staining. PSVue staining (B, B′) shows prominently stained aggregates of cells in the more caudal and medial parts of the forebrain (B). Higher magnifications reveal surprisingly large aggregates of PSVue-positive cells that match the distribution of opaque cells seen at the macroscopic level (B′). Staining for the neuronal marker anti-acetylated β-tubulin shows fibers most prominent in areas of anti-cleaved caspase 3 staining (C, C′, D, D ′) whereas areas of prominent PSVue staining reveal little nerve fiber staining (B, B′, D, D′). This suggests that loss of tubulin correlates with the appearance of phosphatidylserine on the surface of dying neurons. Bar indicates 100 μm.

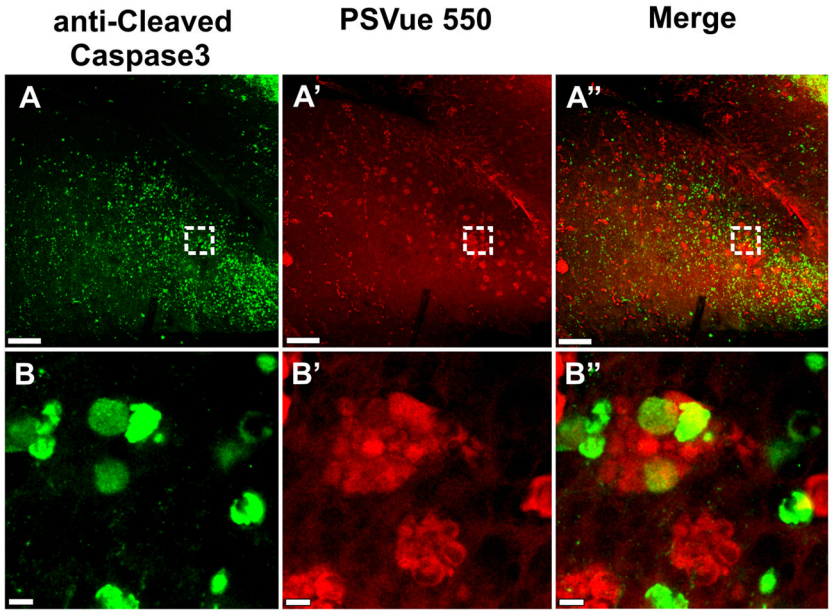

Fig. 8.

Staining with anti-cleaved caspase 3 and PSVue of the cerebellum of an E12.5 *Foxg1-cre:: Dicer1* $^{f/f}$ CKO mouse shows widespread caspase 3 upregulation throughout the cerebellum (A). Staining for phosphatidylserine with PSVue shows an overlapping distribution of cells in possibly different stages of degeneration (A′, A″). Higher power images show that anti-cleaved caspase 3-positive cells are mostly individually distributed (B) whereas the PSVue labeled cells are mostly aggregated (B′). Combined imaging shows that either labeling is rarely overlapping with the other, or if they do, both stain weakly (B″). This suggests that either stain reveals cells at different stages of degeneration with the PSVue dye showing presumably cells already ingested by activated microglia cells that turned into macrophages. Bar indicates 100μm A-A″ and 5μm B-B″.

Table 1

Reduction in eye size

	WT	*Foxg1-cre::Dicer1* $^{f/f}$	% Reduction
E12.5 radius	245	241	1.6%
E12.5 volume	62	59	4.8%
E14.5 radius	465	303	34.8%
E14.5 volume	421	117	72.2%
E18.5 radius*	1197 +/− 217	636.5+/− 150.5	46.8%
E18.5 volume*	7184	1080	84.9%

* indicates that average values from two WT and two CKO eyes were used in this table at E18.5.

+/− indicates standard deviations for radius. Values for radius and volume are in μm and μm^3, respectively.